Mineralogical and Geochemical Characteristics of Porphyry-Fertile Plutons: Guichon Creek, Takomkane and Granite Mountain Batholiths, South-Central British Columbia (NTS 092I, P, 093A, B)

F. Bouzari, Mineral Deposit Research Unit, The University of British Columbia, Vancouver, BC, fbouzari@eos.ubc.ca

C.J.R. Hart, Mineral Deposit Research Unit, The University of British Columbia, Vancouver, BC

T. Bissig, Mineral Deposit Research Unit, The University of British Columbia, Vancouver, BC

G. Lesage, Mineral Deposit Research Unit, The University of British Columbia, Vancouver, BC

Introduction

Distinguishing metal-fertile from barren plutons provides a significant advantage for exploration for porphyry Cu deposits, particularly in British Columbia (BC), where many porphyry systems occur within or around the edges of large batholiths. The fundamental relationship of porphyry Cu (Au, Mo) deposits with bodies of intrusive rocks is well established (e.g., Sillitoe, 1973, 2010), but distinguishing metal-fertile from barren plutons remains a significant challenge for exploration. This is largely because porphyry-related intrusive rocks are common in convergent-margin settings, yet very few host ore deposits. Information that contributes such *a priori* knowledge provides guidance early in the exploration process to make decisions more effectively and efficiently, in order to focus exploration resources on the most prospective targets. This research project, therefore, provides tools and strategies that emphasize porphyry fertility in the BC context.

The formation of porphyry Cu deposits is fundamentally controlled by magmatic processes that generate hydrothermal fluids enriched in metals, Cl and S (e.g., Dilles and Einaudi, 1992). These buoyant fluids are focused in cupolas above the batholiths at shallow depths of 2–4 km, which leads to the formation of porphyry Cu deposits. In many districts, large deposits are hosted within or adjacent to the large plutons that form part of the mineralizing system. These plutons host mineralogical evidence that records fertility characteristics, such as presence of Cl and S, favourable oxidation state and suitable depths of emplacement. The relationship between magmatic processes and ore deposits has long been the focus of ore-deposit research (e.g., Dilles et

al., 2015), but past studies have generally concentrated on the deposit scale. This project investigates district- to batholith-scale porphyry fertility in the Guichon Creek, Takomkane and Granite Mountain batholiths (Figure 1), which will provide a level of assessment not previously documented in BC.

Field and Laboratory Work

Field and laboratory work focused on the characterization of accessory minerals in various intrusive bodies of three well-documented and mapped batholiths, the Guichon Creek, Takomkane and Granite Mountain batholiths, located in south-central BC (Figure 1). In total, 113 rock samples were collected: 52 from Guichon Creek, 35 from Takomkane and 26 from Granite Mountain. Samples were collected from various intrusive phases that constitute each batholith. Samples were disaggregated using an electric-pulse disaggregator (EPD) at Overburden Drilling Management Limited (Nepean, Ontario) to break the rock along mineral-grain boundaries, providing a larger number of unbroken mineral grains. Subsequently, mineral separation was performed at the Mineral Deposit Research Unit (MDRU), The University of British Columbia using Frantz® magnetic separation and heavy liquids.

Mineral grains were handpicked, mounted and polished in preparation for electron-probe microanalysis (EPMA) and trace-element laser-ablation inductively coupled plasma–mass spectrometry (LA-ICP-MS) at The University of British Columbia. More than 3000 grains of apatite, titanite, zircon and amphibole were separated. These grains were studied and characterized by binocular, petrographic and cathodoluminescence (CL) microscopy, as well as by scanning electron microscope (SEM). Properties such as colour, shape, inclusion populations, zoning and replacements were documented for each grain. Mineral grains were then analyzed by EPMA for major elements and some trace ele-
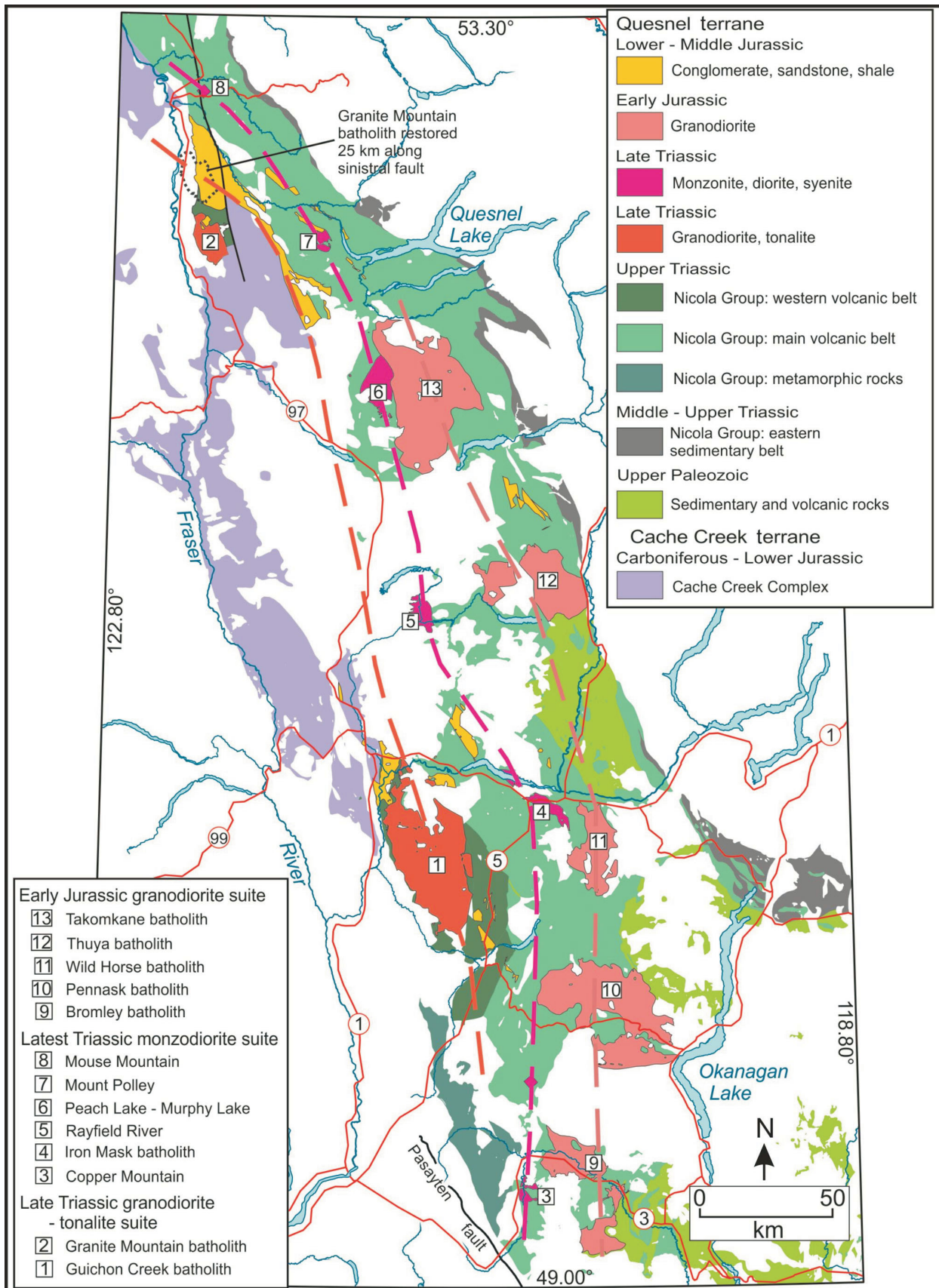
Figure 1. Simplified geology of south-central British Columbia, showing the location of major plutonic bodies. Dashed lines illustrate parallel belts of calcalkaline or alkaline plutons that show progressive younging from west to east (from Schiarizza, 2015).

ments. Subsequently, the same grains were analyzed by LA-ICP-MS for a full trace-element characterization.

Whole-rock samples were analyzed for major and trace elements at Bureau Veritas Minerals (Vancouver, BC; formerly Acme Analytical Laboratories Ltd.), to characterize the geochemical signature of each intrusive unit and to compare the mineral chemistry with whole-rock chemistry. Polished thin sections were prepared from representative samples for petrography.

This paper summarizes initial mineral-grain chemistry results from selected samples based on EPMA and LA-ICP-MS.

Guichon Creek Batholith

The Late Triassic Guichon Creek batholith (Figure 2) is a north-trending, approximately 65 by 30 km body that intruded and thermally metamorphosed the Upper Triassic Nicola Group basaltic to andesitic volcanic and volcaniclastic rocks (Casselman et al., 1995) that form part of the Quesnel terrane. The batholith is composite, with diorite and quartz diorite border phases flanking a younger granodiorite phase in the centre (Casselman et al., 1995; Byrne et al., 2013). These phases, from the margins inward, are: the Border phase, the Highland Valley phases (consisting of Guichon and Chataway subphases), the Bethlehem phases (consisting of Bethlehem and Skeena subphases) and the Bethsaida phase. The Bethlehem and Skeena subphases and the Bethsaida phase host most of the Highland Valley porphyry Cu-Mo deposits (Valley, Lornex, Highmont, Alwin, Bethlehem and JA). Two mineralization events are recognized: an older event that formed the deposits in the Bethlehem area and was associated with the emplacement of the Bethlehem phase, followed by the formation of the Valley, Lornex and Highmont deposits in conjunction with the emplacement of the Skeena and Bethsaida phases (Byrne et al., 2013).

Takomkane Batholith

The Takomkane batholith (Figure 3) is a large (40 by 50 km) Late Triassic–Early Jurassic composite intrusive body that hosts several mineralized centres. It intrudes the Spout Lake pluton and is cut by Early Jurassic ultramafic–mafic
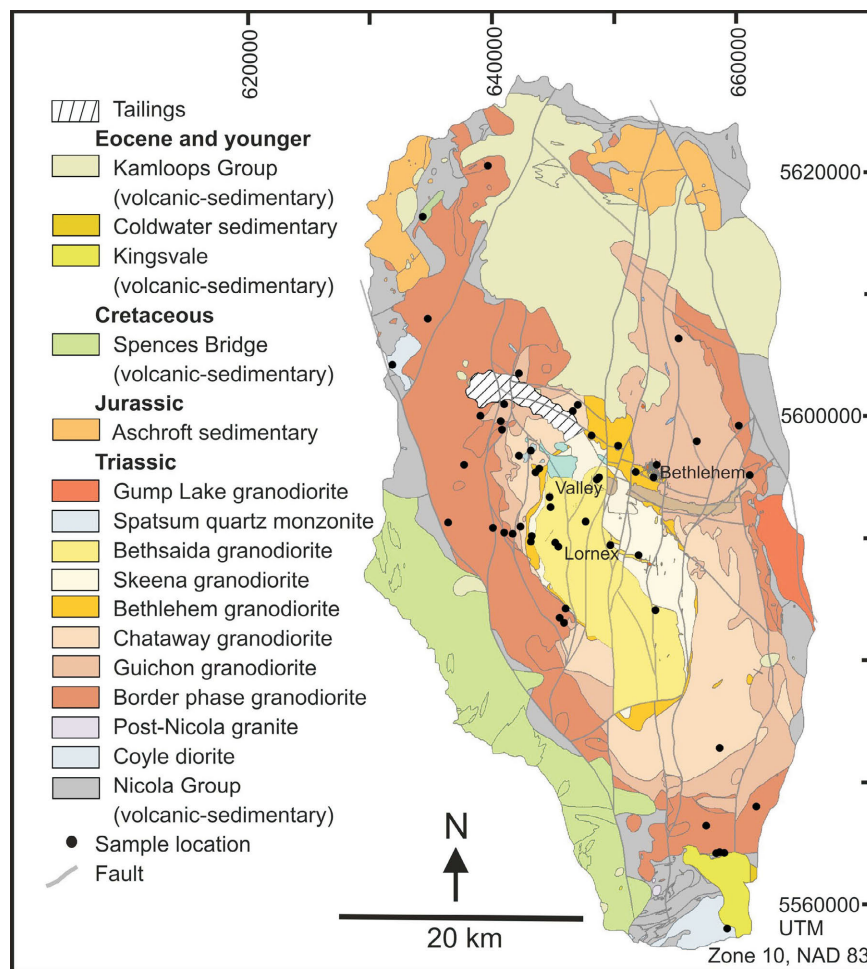

Figure 2. Simplified geology of the Guichon Creek batholith, showing the main intrusive units and sample locations (summarized and redrafted after McMillan et al., 2009).
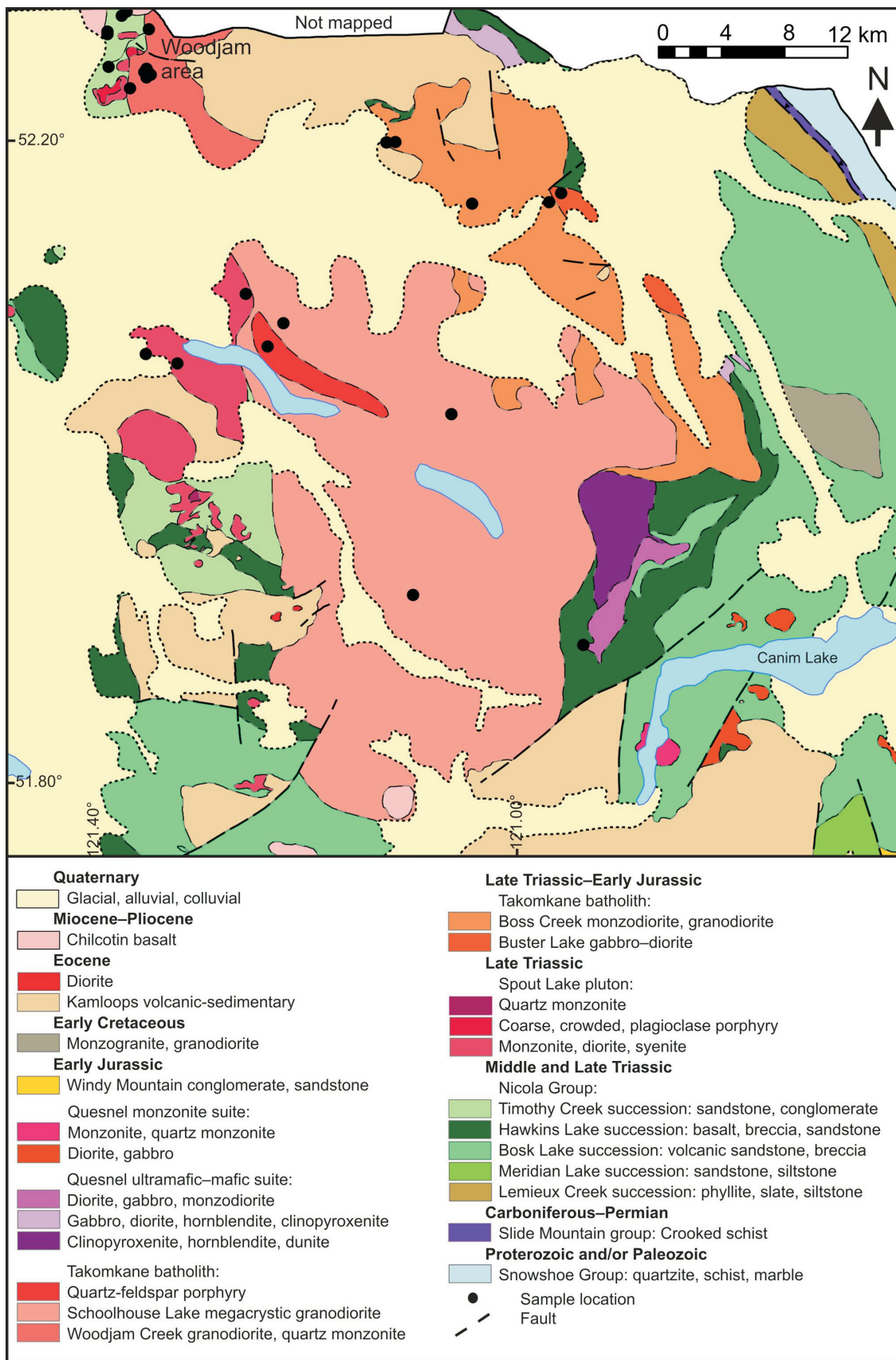
Figure 3. Simplified geology of the Takomkane batholith, showing the main intrusive units and sample locations (summarized and redrafted after Schiarizza et al., 2013).

plutons and the Early Cretaceous Boss Mountain Mine stock. The Takomkane batholith consists of two major units: the Late Triassic–Early Jurassic Boss Creek unit and the Early Jurassic megacrystic Schoolhouse Lake unit. A smaller-volume unit of quartz-feldspar porphyry occurs within the Schoolhouse Lake unit. The Woodjam Creek unit is texturally distinct but compositionally similar to the Schoolhouse Lake unit and forms the northwestern part of the batholith (Schiarizza et al., 2009).

Several small Cu showings occur within the Spout Lake pluton and, to a lesser extent, within the Boss Creek and Schoolhouse units (Schiarizza et al., 2009). However, economically more significant Cu-Mo-Au porphyry mineralization occurs along the northwestern boundary of the batholith in the Woodjam area (Megabuck, Takom, Southeast and Deerhorn deposits). These deposits are hosted within the Woodjam Creek unit or in small porphyry dikes and adjacent volcanic rocks. The Takomkane batholith records a magmatic evolution lasting 11 m.y., with three separate mineralizing events identified at Woodjam (del Real, 2015). The presence of Cu-Au and Cu-Mo deposits, together with the regional northwest tilting of geological units, provides an insight into different levels of exposure and potentially subtle geochemical variations within the intrusive bodies.

Granite Mountain Batholith

The Late Triassic Granite Mountain batholith (18 by 10 km) occurs near McLeese Lake in south-central BC and hosts the Gibraltar porphyry Cu-Mo mine (Figure 4). The batholith is subdivided into three main units, from south-west to northeast: Border phase diorite to quartz diorite, Mine phase tonalite and Granite Mountain phase leucocratic tonalite. The Burgess Creek stock (Panteleyev, 1978), to the northeast, comprises a heterogeneous assemblage of tonalite, quartz diorite and diorite that intrudes the Nicola Group. Panteleyev (1978) considered the stock to be younger than the Granite Mountain batholith, but more recent dating by Schiarizza (2015) has shown that it is 4–5 m.y. older than the adjacent Granite Mountain phase of the batholith. As suggested by Ash et al. (1999), the Burgess Creek stock may represent the border phase part of the batholith.

It was originally thought that the Granite Mountain batholith intruded the Cache Creek terrane (Bysouth et al., 1995). However, mapping by Schiarizza (2015) recognized Nicola Group strata on the northeastern margin of the batholith and suggested that it is more likely a part of the Quesnel terrane. This is also supported by recent interpretation of aeromagnetic data that has assigned the Granite Mountain area to the Quesnel terrane (Sánchez et al., 2015). Thus, the Granite Mountain batholith is correlative with the Late Triassic, calcalkaline Guichon Creek batholith, host to the Highland Valley porphyry Cu-Mo deposits, 250 km to the south-southeast. Mineralization at the Gibraltar mine is hosted in the Mine phase tonalite of the Granite Mountain batholith, but small porphyry-style mineral occurrences are also known in the Border phase and the Granite Mountain phase (Schiarizza, 2015).
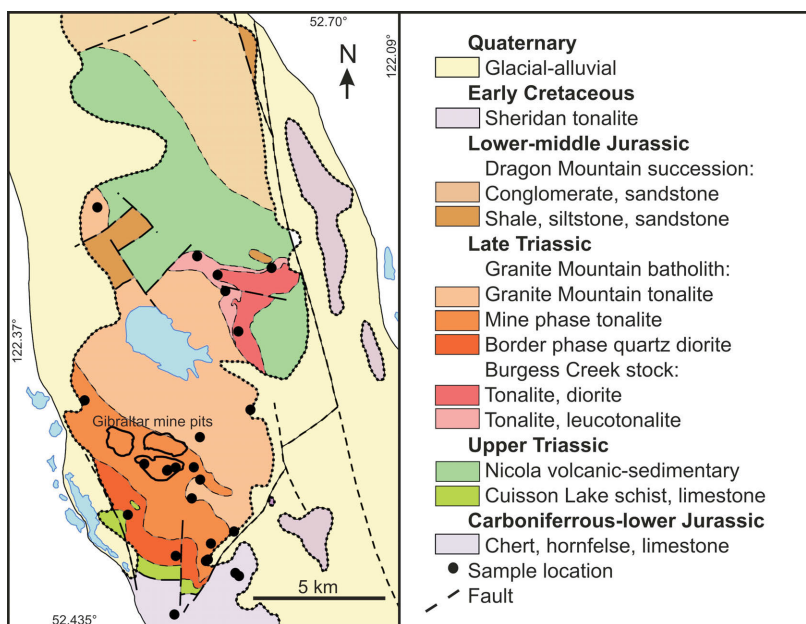

Figure 4. Geology of the Granite Mountain batholith, showing the main intrusive units and sample locations (redrafted after Schiarizza, 2015).

Apatite Chemistry

Trace-element compositions of apatite ($Ca_5(PO_4)_3$ (F,Cl,OH)) have been used to recognize the characteristics of mantle fluids, assimilation, degree of fractionation and the oxidation state of magma (summarized in Bouzari et al., 2016). Zoned magmatic apatite commonly has S-rich cores that abruptly change to S-poor rims, indicating that early SO_4-rich magma evolved to SO_4-poor magma via crystallization of anhydrite (e.g., Streck and Dilles, 1998). Moreover, apatite associated with porphyry Cu deposits is Cl rich (e.g., Roegge et al., 1974). Thus, apatite records the chloride content of the crystalizing melt, which may have played a key role in transporting Cu (Holland, 1972). Mao et al. (2016) used apatite compositions to discriminate their various hostrock and deposit types. Bouzari et al. (2016) showed that apatite luminescence and chemistry can record differing types of hydrothermal alteration in BC porphyry deposits.

Apatite luminescence in the studied samples varied from brown to green and yellow. Apatite grains in largely nonmineralized phases display mostly uniform to zoned brown luminescence (Figure 5a). Some apatite grains have narrow rims of green luminescence or the green luminescence occurs along fractures across the apatite (Figure 5b), suggesting weakly developed zoning or replacement processes. Apatite grains from mineralized rocks have well-developed green luminescence. The green-luminescent apatite typically has darker cores, in most cases a dark brown domain that is zoned outward to green-brown– and green-luminescent apatite (Figure 5c). Apatite grains in mineralized units, particularly the Bethsaida phase of the Guichon Creek batholith, the Woodjam Creek unit of the Takomkane batholith and the Mine phase of the Granite Mountain batholith, display well-developed green luminescence. Locally, the entire apatite grain has green luminescence (Figure 5d). The main exception is the poorly mineralized Schoolhouse Lake unit of the Takomkane batholith, which shows apatite with brown luminescent cores but well-developed green luminescent zones (Figure 5e). Apatite grains from altered-mineralized hostrocks typically display both green and patchy grey luminescence (Figure 5f), reflecting proximal hydrothermal-alteration effects (Bouzari et al., 2016).

Detailed electron-probe microanalyses of several zoned apatite grains show a correlation between luminescence and chemistry. The brown-luminescent cores are S and C rich but with low Fe/Mn ratios. Green-luminescent apatite rims have relatively low concentrations of S and Cl but higher Fe/Mn ratios (Figure 6). In zoned apatite, there is generally a decrease in S and Cl concentrations and an increase in Fe/Mn ratio from the core to rim (see Figure 5c).

Chemical analyses of apatite grains show distinct variations between mineralized and barren phases of the batholiths. In the Bethsaida phase of the Guichon Creek batholith, which is the main host to the Highland Valley porphyry deposits, apatite grains have less Cl and S relative to the Chataway phase. The Cl concentration of apatite in both phases is less than that of apatite in the Guichon phase (Figure 7a). Similarly, apatite from the Mine phase of the Granite Mountain batholith, which is the main host to the Gibraltar deposit, has lower Cl and S concentrations than apatite from the unmineralized Burgess Creek stock (Figure 7b). The Granite Mountain phase shows Cl and S concentrations similar to the Mine phase. The apatite composition of the Takomkane batholith shows some variability. Apatite from the Late Triassic Spout Lake monzodiorite and the Jurassic Woodjam Creek monzogranite has variable Cl and S concentrations from high to low, roughly displaying a trend from high S and Cl values to low values (Figure 7c). Both of these units are the main host to the Cu mineralization, although the known extent of mineralization in the Woodjam Creek is larger than that in the Spout Lake (Schiarizza et al., 2009). The Late Triassic–Early Jurassic Boss Creek monzodiorite and Jurassic Schoolhouse Lake megacrystic granodiorite have apatite with largely moderate to low S and low Cl concentrations. The Boss Creek apatite has uniform brown luminescence, whereas Schoolhouse Lake apatite has locally brown luminescent cores surrounded by green luminescent rims. Both of these units host only a few subeconomic Cu occurrences (Rodeo and Lucy Jack occurrences).

These observations suggest that, in each batholith, the mineralized intrusive bodies evolved from early Cl- and S-rich phases toward phases with less Cl and S. This can be seen in zoned apatite grains, which became progressively depleted in Cl and S from core to rim. Therefore, the apatite from mineralized intrusive bodies displays a depletion trend for Cl and S and commonly has lower concentrations of these elements relative to the barren or less mineralized bodies. Apatite with scattered but low Cl and S concentrations and commonly uniform CL texture, such as those from Boss Creek, suggests a probable low budget of Cl and S in the crystalizing melt. This apatite differs clearly from that in mineralized rock units.

Titanite Chemistry

Titanite ($CaTiSiO_5$) is a common accessory mineral occurring in amounts of about 2–4% in various phases of the studied batholiths. Titanite grains are 1–2 mm, range from colourless to dark brown and locally contain inclusions of an opaque phase, most commonly ilmenite. Less commonly, inclusions of apatite and quartz are also noted (Figure 8a). Titanite textures under SEM vary from uniform to zoned, and more rarely display irregular mottled rims. Titanite is a robust and stable phase in a magmatic system and

can incorporate geochemically important trace elements into its structure, thus providing a powerful tool for petrogenetic studies (e.g., Kowallis, 1997; Piccoli et al., 2000) and studies of ore deposit–related alteration processes (e.g., Che et al., 2013; Celis, 2015). Electron-microprobe data were used to calculate mineral formulas based on five oxygens in the ideal titanite formula, ABOTO4, where the A site is filled by Ca^{2+}, Mn^{2+}, Na^+, K^+ and REE^{3+}, the B site is filled by Ti^{4+}, Fe^{3+} and Al^{6+}, and the T site is filled by Si^{4+} and Al^{4+}.
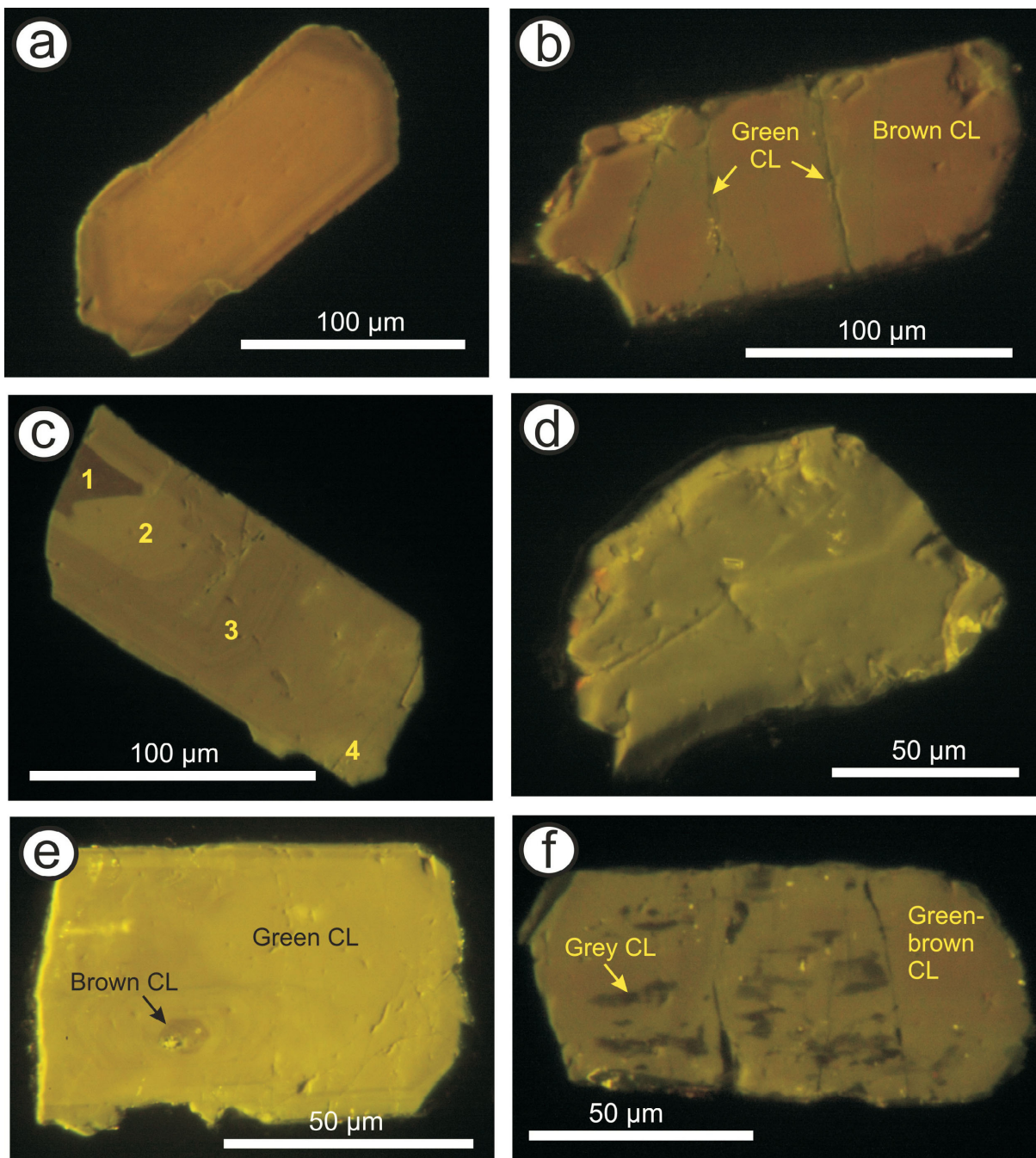

Figure 5. Cathodoluminescence images of apatite grains from the Guichon Creek, Takomkane and Granite Mountain batholiths: **a)** zoned apatite with brown luminescence from the Spout Lake pluton, Takomkane batholith; **b)** apatite from the Granite Mountain phase of the Granite Mountain batholith with brown luminescence and weak green luminescence developed along fractures; **c)** zoned apatite from the Woodjam Creek unit of the Takomkane batholith, showing a core with brown luminescence and a rim with green luminescence; numbers represent location of spots analyzed by EPMA (see Figure 6); **d)** apatite from the Bethsaida phase of the Guichon Creek batholith, showing green luminescence; **e)** apatite from the Schoolhouse Lake unit of the Takomkane batholith with a brown luminescent core surrounded by yellow-green luminescent apatite; **f)** apatite from the altered and mineralized Mine phase of the Granite Mountain batholith with green luminescence, as well as remnants of brown luminescence overprinted by grey luminescence. Abbreviations: CL, cathodoluminescence; EPMA, electron-probe microanalysis.

The chemical composition of titanite from the Guichon Creek batholith shows a correlation between rock type and Fe, Al and Mn concentrations, specifically a positive correlation between Fe/Al and Mn/Ca ratios. More importantly, titanite in the Bethsaida and Skeena granodiorite (host to the mineralization) has the highest Fe/Al and Mn/Ca ratios, whereas titanite in the other phases of batholith has lower Fe/Al and Mn/Ca (Figure 9a). In fact, the Fe/Al and Mn/Ca ratio increases from the older border phase to the (younger) central mineralized phase (Bethsaida) of the batholith.

Titanite from the Takomkane batholith has similar variations. The mineralized Woodjam Creek granodiorite has high Fe/Al and moderate Mn/Ca ratios. Titanite in the older Boss Creek unit and the younger Schoolhouse Lake unit has lower Fe/Al relative to that in the Woodjam Creek unit but similar moderate Mn/Ca (Figure 9b). The quartz-feldspar porphyry, which occurs as a small body inside the Schoolhouse Lake unit, has titanite with similar Fe/Al and Mn/Ca ratios, but some grains have ratios that are distinctly higher than those in the Woodjam Creek unit. The Late Triassic Spout Lake monzodiorite has Fe/Al and Mn/Ca ratios similar to those in the Schoolhouse Lake unit. The Quesnel diorite, which cuts the Takomkane batholith units, has ti-

tanite with low Mn/Ca and moderate Fe/Al ratios. Overall, Takomkane titanite, similar to Guichon Creek titanite, shows a positive correlation between Fe/Al and Mn/Ca ratios, with the mineralized unit showing high Fe/Al compositional ratios. However, unlike the Guichon Creek batholith, that shows a single trend of Fe/Al and Mn/Ca ratios for titanite, the Takomkane batholith shows at least two distinct trends, possibly reflecting more complex intrusive relationships.
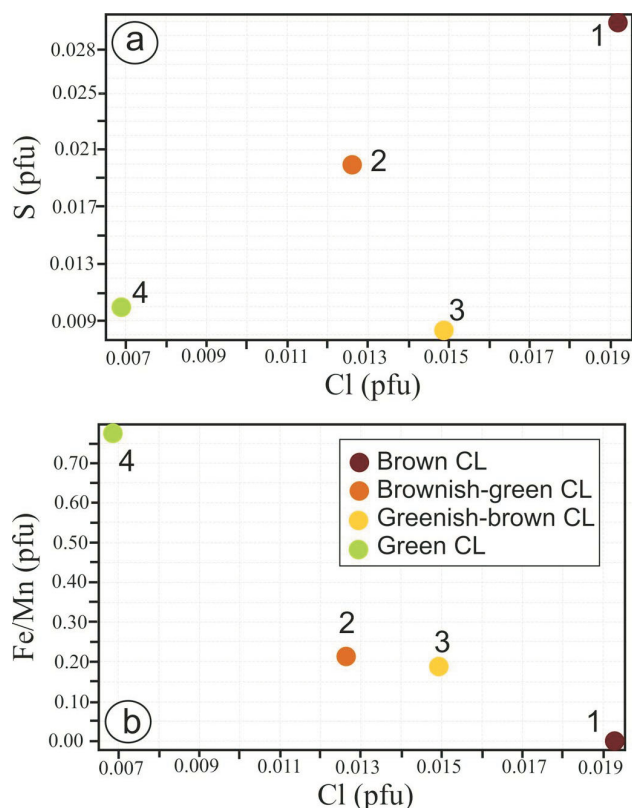

Figure 6. Binary diagram showing correlation of apatite luminescence in a single zoned apatite grain from the Woodjam Creek unit of the Takomkane batholith with Cl and S concentrations (see Figure 5c for location of analyzed spots). Abbreviations: CL, cathodoluminescence; pfu, per formula unit.
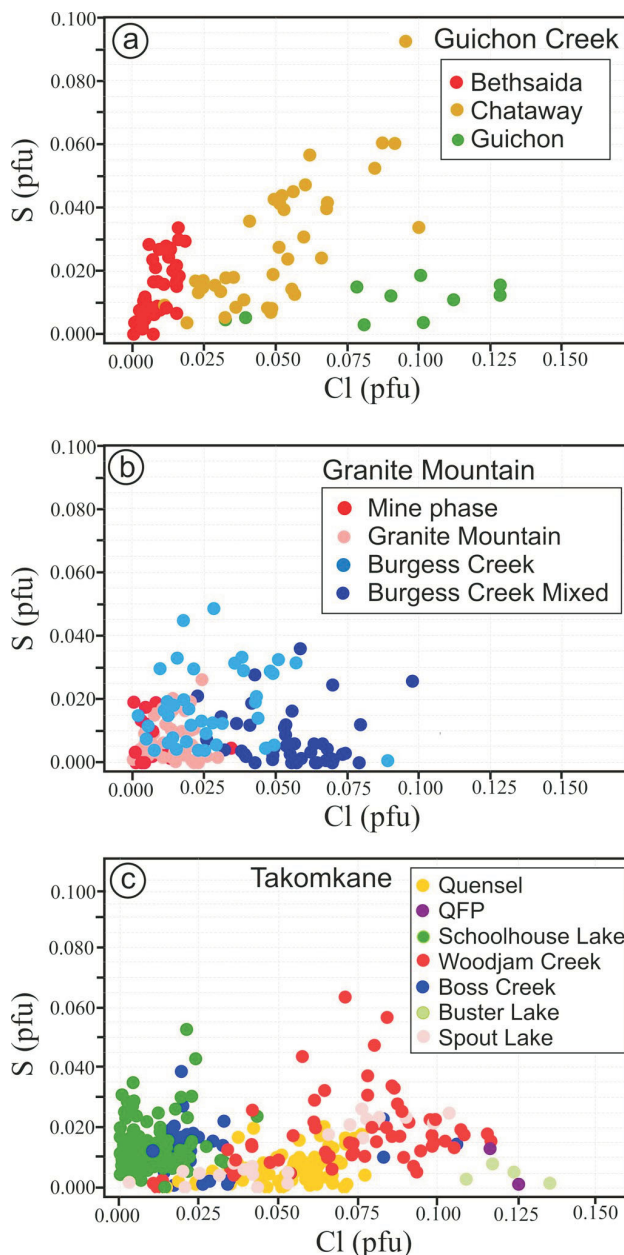
Figure 7. Binary diagrams of apatite compositions in various mineralized and barren pluton phases of the Guichon Creek, Takomkane and Granite Mountain batholiths; Cl and S values are calculated per formula unit (pfu). Abbreviation: QFP, quartz-feldspar porphyry.
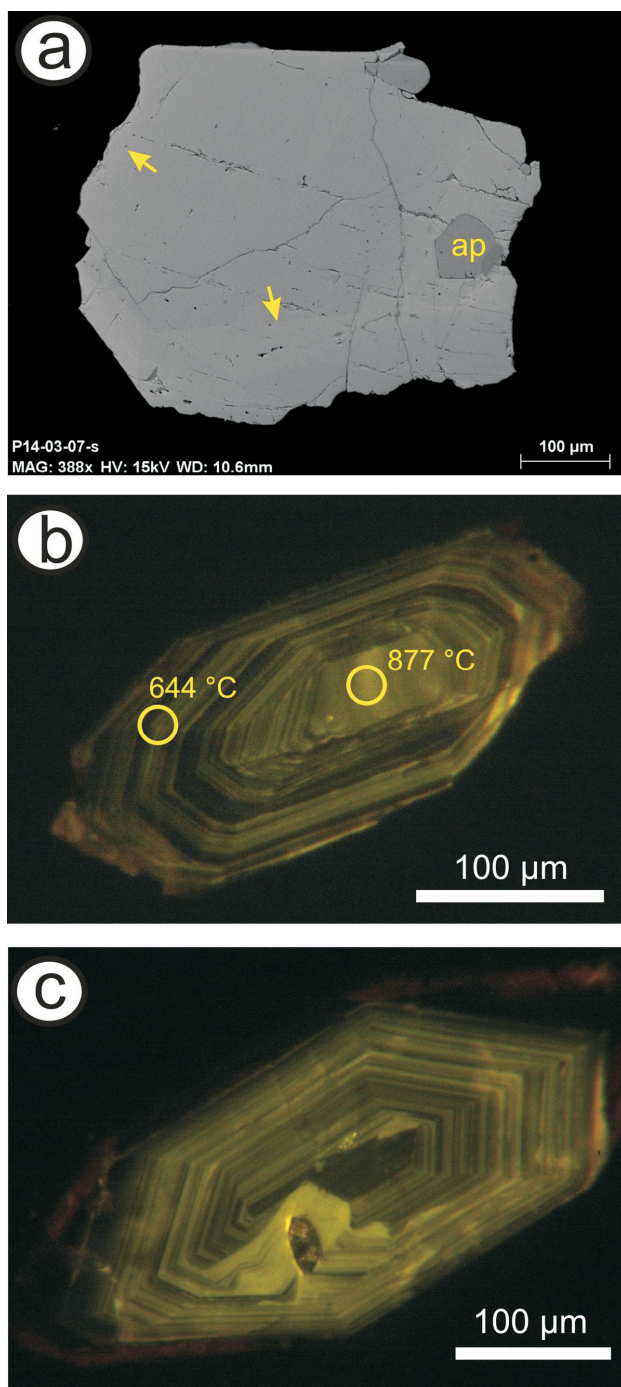
Figure 8. a) Scanning electron microscope image of a zoned titanite grain from the Bethlehem phase of the Takomkane batholith; the rim shown by arrows has higher Fe/Al and Mn/Ca ratios relative to the core. **b)** Cathodoluminescence image of a zircon grain from the quartz-feldspar porphyry unit of the Takomkane batholith, showing oscillatory zoning and, on the basis of Ti-in-zircon thermometry, a lower crystallization temperature at the rim; yellow circles represent areas analyzed by LA-ICP-MS. **c)** Cathodoluminescence image of zircon from the Schoolhouse Lake unit of the Takomkane batholith, showing oscillatory zoning with some irregularity causing termination of some zones, especially near a mineral inclusion.

Zircon Chemistry

Zircon ($ZrSiO_4$) is a geochemically robust mineral that records orthomagmatic chemical compositions that influence formation of porphyry Cu deposits. Zircon trace-element behaviour, as recorded during its growth, can be used to examine crystal fractionation, crustal assimilation and magma mixing. Zircon incorporates a suite of lithophile elements, including rare-earth elements (REE), U, Th and Hf, in concentrations that are dependent upon the pressure, temperature and composition of the magma (Hanchar and Watson, 2003). In addition, the Ti-in-zircon geothermometer can determine zircon-crystallization temperatures (Ferry and Watson 2007). Zircon is also a sensitive indicator of the magmatic oxidation state because of its multivalent Ce and Eu contents. Investigation by Ballard et al. (2002) and more recently by Shen et al. (2015) correlated the relative Ce^{4+}/Ce^{3+} in zircon with the oxidation state of barren and Cu-mineralized intrusive rocks in northern Chile and central Asia. Dilles et al. (2015) showed similar relationships for porphyry deposits in Chile using the Eu concentration in zircon and suggested that small negative Eu anomalies ($Eu_N/Eu_N^* = 0.4$) indicate oxidizing magmatic conditions that reflect oxidation due to SO_2 degassing from magmas.

Zircon typically forms 100–500 μm long grains with complex internal oscillatory and sector zonation; in some cases, the grains have inherited cores. Cathodoluminescence imaging was used to characterize zircon grains. Oscillatory zoning typically forms fine concentric zones of dark- and light-coloured domains (Figure 8b). The zoning, in some cases, becomes irregular and new growth zones may crosscut older zones (Figure 8c), probably due to chemical disequilibrium or a pronounced change in temperature. Results from LA-ICP-MS analysis of selected Takomkane batholith rock samples demonstrate the application of zircon chemistry to BC porphyry-fertility studies.

Results of the calculated Ti-in-zircon temperature, corrected to an activity for TiO_2 of ~0.7, are plotted against Hf concentration in Figure 10a. Despite some scatter in the data, probably due to analytical uncertainties and small variations in the activity of TiO_2 in melt, Figure 10a illustrates that the Hf content in zircon increases with a decrease in Ti-in-zircon temperature, as has been previously documented in other felsic melts (e.g., Claiborne et al., 2010). Zircons from the Boss Creek unit show variable temperatures ranging from 950°C to below 650°C, whereas the Schoolhouse Lake unit has temperatures above 850°C (Figure 10a). Zircons from the mineralized Woodjam Creek granodiorite and the late quartz-feldspar porphyry unit have modelled Ti-in-zircon temperatures of 750–650°C, consistent with zircon crystallization in near-eutectic conditions close to the solidus of hydrous granite. Zircons from the youngest smaller unit of quartz-feldspar
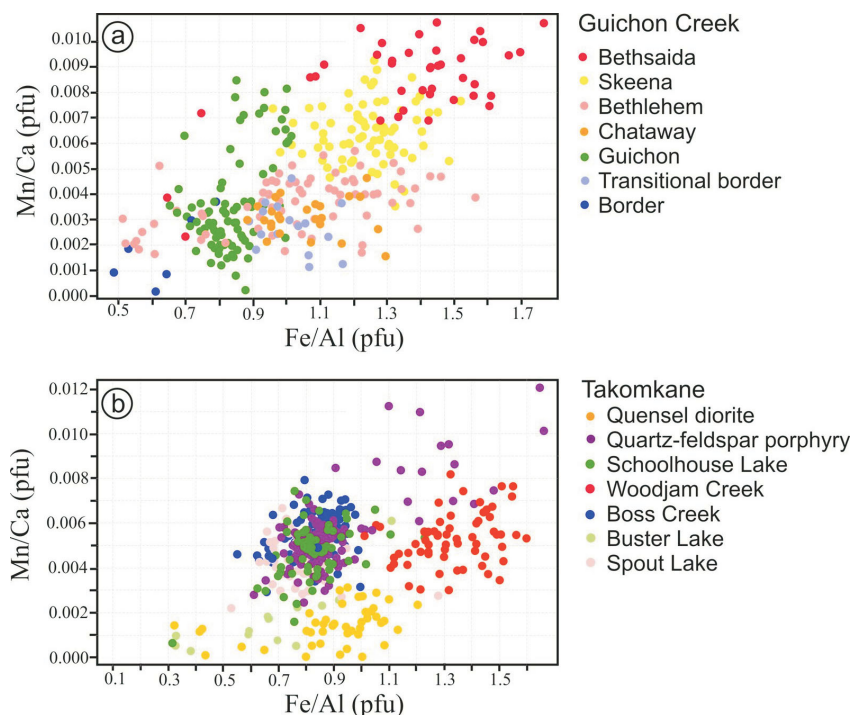
Figure 9. Binary diagrams of titanite compositions in various mineralized and barren pluton phases of **a)** the Guichon Creek batholith, showing that the Bethsaida and Skeena phases have high Fe/Al and Mn/Ca; and **b)** the Takomkane batholith, showing that the Woodjam Creek unit has high Fe/Al but moderate Mn/Ca.

porphyry have a temperature range similar to or less than that of the Woodjam Creek unit.

The chondrite-normalized negative Eu anomaly (Eu_N/Eu_N*, where $Eu_N* = (Sm_N \times Gd_N)^{1/2}$) of zircon has been used to characterize the fertility of igneous rocks (Ballard et al., 2002; Dilles et al., 2015). Chemical compositions of zircon grains from the Takomkane batholith indicate that the unmineralized Boss Creek unit has a more pronounced Eu anomaly ($Eu_N/Eu_N* <0.35$) compared to the other rock suites. Zircons from the mineralized Woodjam Creek unit have relatively small negative Eu anomalies (mostly $Eu_N/Eu_N* >0.35$). The younger phases of batholith, Schoolhouse Lake and the quartz-feldspar porphyry unit, are both similar to the Woodjam Creek unit in displaying $Eu_N/Eu_N* <0.35$, but these phases have a larger range of Eu_N/Eu_N* values (Figure 10b).

Discussion

The results of this study suggest that the chemical compositions of apatite, titanite and zircon can be used to characterize porphyry-fertile intrusive rocks. Porphyry-fertile plutons contain apatite that becomes progressively depleted in Cl and S, but enriched in Fe relative to Mn, during crystallization. The depletion in S is attributed to the evolution of an early magma that is oxidizing and SO_4 rich to a melt that is SO_4 poor as a result of crystallization of anhydrite (Streck and Dilles, 1998). The increase in the Fe/Mn ratio in apa-
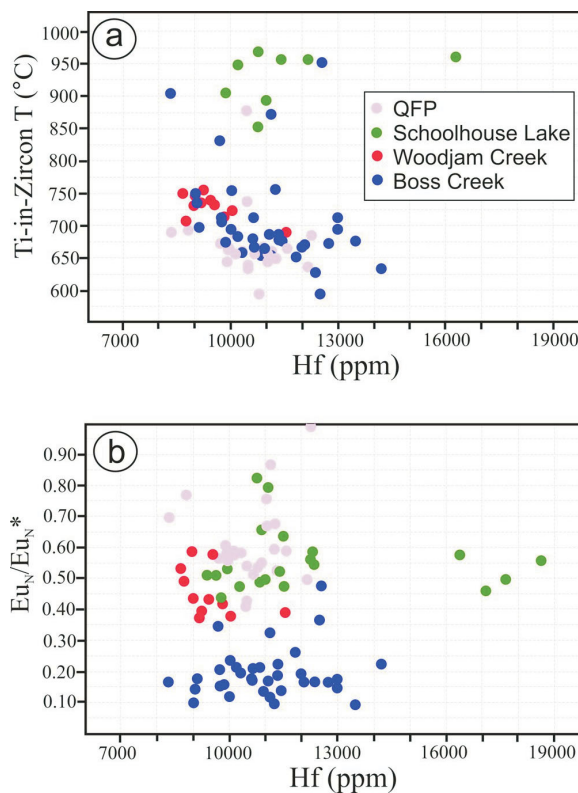

Figure 10. Rare-earth element concentrations in zircon from the Takomkane batholith: **a)** Ti-in-zircon temperature versus Hf concentration, assuming a melt activity for TiO_2 of ~0.7, calculated after Ferry and Watson (2007); **b)** zircon Eu anomaly (Eu_N/Eu_N*) versus Hf concentration. Abbreviation: QFP, quartz-feldspar porphyry.

tite, which is largely responsible for green luminescence, is also interpreted to be controlled by magmatic evolution toward a higher oxidation state. Further cooling of the melt caused saturation in a water-rich fluid phase, and probably the breakdown of crystalline anhydrite and the release of SO_2 to a vapour phase (Dilles et al., 2015). The depletion in both Cl and S of apatite from the mineralized pluton provides evidence for degassing of SO_2-rich magmatic volatiles from SO_4-rich melts. These Cl- and S-rich volatiles generated from such fertile plutons are capable of carrying Cu and producing porphyry Cu ores.

The change of oxidation state is also recognized from the titanite chemistry. Titanite from the mineralized pluton has high Fe/Al, attributed to an increase in oxygen fugacity that controls the abundance of Fe^{3+} substituting for Ti in the B site (Kowallis, 1997). The same conditions were probably responsible for an increase of Mn substituting for Ca in the A site. Evidence from ilmenite in the cores of titanite and higher Fe/Al and Mn/Ca in the rims, also suggest that the mineralized plutons became progressively oxidized over time.

Titanium-in-zircon temperatures calculated for the mineralized units indicate that these magmas were largely crystalized at 750–650°C in near-eutectic conditions close to the solidus of hydrous granite. These data provide additional information about the conditions for metal and S behaviour as they are partitioned into the hydrothermal phase, rather than incorporated into earlier-formed minerals or forming magmatic sulphide (Burnham and Ohmoto, 1980; Candela, 1986). Barren or weakly mineralized plutonic phases show evidence of the initiation of crystallization at higher temperature compared to fertile phases.

Zircon REE compositions indicate that fertile granitic bodies have small negative Eu anomalies (EuN/EuN* =0.35). This reflects 1) high water content and consequent suppression of early plagioclase crystallization (e.g., Ballard et al., 2002) and 2) late magmatic oxidation resulting in the loss of SO_2-rich magmatic-hydrothermal ore fluids during late-stage crystallization of granite (Dilles et al., 2015). The smaller Eu anomalies observed in zircons from mineralized intrusions compared to nonmineralized intrusions may result from suppression of plagioclase crystallization at high pressure and water content (Richards et al., 2012), or they could be due to the higher oxidation state of melts (e.g., Dilles et al., 2015). However, evidence from the Fe/Al ratios in titanite independently suggests higher oxidation state, which is consistent with only moderate Eu anomalies in the zircons of fertile intrusions. Moreover, S and Cl depletion in apatite indicates degassing of SO_2-rich magmatic volatiles, thus supporting the required oxidation state.

This study shows that apatite, titanite and zircon can provide tools to characterize fertility factors in plutonic rocks, in particular Cl and S contents, temperature and oxidation state. The use of these three indicator minerals together provides a means of assessing the Cu fertility of plutons.

References

Ash, C.H., Rydman, M.O., Payne, C.W. and Panteleyev, A. (1999): Geological setting of the Gibraltar mine, south-central British Columbia (93B/8, 9); *in* Exploration and Mining in British Columbia 1998, BC Ministry of Energy and Mines, BC Geological Survey, p. A1–A15.

Ballard, J.R., Palin, J.M. and Campbell, I.H. (2002): Relative oxidation states of magmas inferred from Ce(IV)/Ce(III) in zircon: application to porphyry copper deposits of northern Chile; Contributions to Mineralogy and Petrology, v. 144, p. 347–364.

Bouzari, F., Hart, C.J.R., Bissig, T. and Barker, S. (2016): Hydrothermal alteration revealed by apatite luminescence and chemistry: a potential indicator mineral for exploring covered porphyry copper deposits; Economic Geology, v. 111, p. 1397–1410, URL <http://econgeol.geoscienceworld.org/content/111/6/1397> [November 2016].

Burnham, C.W. and Ohmoto, H. (1980): Late-stage processes of felsic magmatism; *in* Granitic Magmatism and Related Mineralization, S. Ishihara and S. Takenouchi, S. (ed.), Mining Geology, Special Issue 8, p. 1–11.

Byrne, K., Stock, E., Ryan, J., Johnson, C., Nisenson, J., Alva Jimenez, T., Lapointe, M., Stewart, H., Grubisa, G. and Sykora, S. (2013): Porphyry Cu-(Mo) deposits in the Highland Valley district, south-central British Columbia; *in* Porphyry Systems of Central and Southern BC, Tour of Central BC Porphyry Deposits from Prince George to Princeton, J. Logan. and T. Schroeter (ed.), Society of Economic Geologists, Field Guidebook Series, v. 44, p. 99–116.

Bysouth, G.D., Campbell, K.V., Barker, G.E. and Gagnier, G.K. (1995): Tonalite trondhjemite fractionation of peraluminous magma and the formation of syntectonic porphyry copper mineralization, Gibraltar mine, central British Columbia; *in* Porphyry Deposits of the Northwestern Cordillera of North America, T.G. Schroeter (ed.), Canadian Institute of Mining, Metallurgy and Petroleum, Special Volume 46, p. 201–213.

Candela, P.A. (1986): The evolution of aqueous vapor from silicate melts: effect on oxygen fugacity; Geochimica et Cosmochimica Acta, v. 50, p. 1205–1211.

Casselman, M.J., McMillan, W.J. and Newman, K.M. (1995): Highland Valley porphyry copper deposits near Kamloops, British Columbia: a review and update with emphasis on the Valley deposit; *in* Porphyry Deposits of the Northwestern Cordillera of North America, T.G. Schroeter (ed.), Canadian

Institute of Mining and Metallurgy, Special Volume 46, p. 161–191.

Celis, M.A. (2015): Titanite as an indicator mineral for alkalic Cu-Au porphyry deposits in south-central British Columbia; M.Sc. thesis, The University of British Columbia, 247 p.

Che, X.D., Linnen, R.L., Wang, R.C, Groat, L.A. and Allison, A.B. (2013): Distribution of trace and rare earth elements in titanite from tungsten and molybdenum deposit in Yukon and British Columbia, Canada; The Canadian Mineralogist, v. 51, p. 415–438.

Claiborne, L.L., Miller, C.F. and Wooden, J.L. (2010): Trace element composition of igneous zircon: a thermal and compositional record of the accumulation and evolution of a large silicic batholith, Spirit Mountain, Nevada; Contributions to Mineralogy and Petrology, v. 160, p. 511-531.

del Real, I. (2015): Geology, alteration, mineralization and magmatic evolution of the Southeast Zone (Cu-Mo) and Deerhorn (Cu-Au) porphyry deposits, Woodjam, central British Columbia, Canada; M.Sc. thesis, The University of British Columbia, 315 p.

Dilles, J.H. and Einaudi, M.T. (1992): Wall-rock alteration and hydrothermal flow paths about the Ann-Mason porphyry copper deposit, Nevada: a 6-km vertical reconstruction; Economic Geology, v. 87, p. 1963–2001.

Dilles, J.H., Kent, A.J.R., Wooden, J.L., Tosdal, R.M., Koleszar, A., Lee, R.G. and Farmer, L.P. (2015): Zircon compositional evidence for sulfur-degassing from ore-forming arc magmas; Economic Geology, v. 110, p. 241–251

Ferry, J.M., and Watson, E.B. (2007): New thermodynamic models and revised calibrations for the Ti-in-zircon and Zr-in-rutile thermometers; Contributions to Mineralogy and Petrology, v. 154, p. 429–437.

Hanchar, J.M. and Watson, E.B. (2003): Structure and chemistry of zircon and zircon group minerals; in Zircon, J.M. Hanchar and P.W.O. Hoskin (ed.), Reviews in Mineralogy and Geochemistry, v. 53, p. 89–112

Holland, H.D. (1972): Granites, solutions, and base metal deposits; Economic Geology, v. 67, p. 281–301.

Kowallis, B.J. (1997): Compositional variations in titanite; Geological Society of America, Abstracts with Programs, v. 29, p. 402.

Mao, M., Rukhlov A.S., Rowins, S.M., Spence, J. and Coogan, L.A. (2016): Apatite trace element compositions: a robust new tool for mineral exploration; Economic Geology, v. 111, p. 1187–1222, URL <http://econgeol.geoscienceworld.org/content/111/5/1187> [November 2016].

McMillan, W.J., Anderson, R.G., Chan, R. and Chow, W. (2009): Geology and mineral occurrences (MINFILE), the Guichon Creek Batholith and Highland Valley porphyry copper district, British Columbia; Geological Survey of Canada, Open File 6079, 2 maps, URL <http://geogratis.gc.ca/api/en/nrcan-rncan/ess-sst/78e93fdd-50d0-5877-a024-310362144149.html> [November 2016].

Panteleyev, A. (1978): Granite Mountain project (93B/8); in Geological Fieldwork 1977, BC Ministry of Energy and Mines, BC Geological Survey, Paper 1977-1, p. 39–42.

Piccoli, P., Candela, P. and Rivers, M. (2000): Interpreting magmatic processes from accessory phases: titanite – a small-scale recorder of large-scale processes; Transactions of the Royal Society of Edinburgh, Earth Sciences, v. 91, p. 257–267.

Richards, J.P., Spell, T., Rameh, E., Razique, A. and Fletcher, T. (2012): High Sr/Y magmas reflect arc maturity, high magmatic water content, and porphyry Cu±Mo±Au potential: examples from the Tethyan arcs of central and eastern Iran and western Pakistan; Economic Geology, v. 107, p. 295–332.

Roegge, J.S., Logsdon, M.J., Young, H.S., Barr, H.B., Borcsik, M. and Holland, H.D. (1974): Halogens in apatite from the Providencia area, Mexico; Economic Geology, v. 69, p. 229–240.

Sánchez, M.G., Bissig, T. and Kowalcyzk, P. (2015): Toward an improved basis for beneath-cover mineral exploration in the QUEST area, central British Columbia: new structural interpretation of geophysical and geological datasets (NTS 093A, B, G, H, J, K, N); in Geoscience BC Summary of Activities 2014, Geoscience BC, Report 2015-1, p. 53–62, <http://www.geosciencebc.com/i/pdf/Summaryof Activities2014/SoA2014_Sanchez.pdf> [November 2016].

Schiarizza, P. (2015): Geological setting of the Granite Mountain batholith, south-central British Columbia; in Geological Fieldwork 2014, BC Ministry of Energy and Mines, BC Geological Survey, Paper 2015-1, p. 19–39, <http://www.empr.gov.bc.ca/Mining/Geoscience/Publications Catalogue/Fieldwork/Documents/2014/02_Schiariz za.pdf> [November 2016].

Schiarizza, P., Bell, K. and Bayliss, S. (2009): Geology and mineral occurrences of the Murphy Lake area, south-central British Columbia (NTS 093A/03); in Geological Fieldwork 2008, BC Ministry of Energy and Mines, BC Geological Survey, Paper 2009-1, p. 169–188, <http://www.em pr.gov.bc.ca/Mining/Geoscience/PublicationsCatalogue/ Fieldwork/Documents/2008/15_Schiarizza.pdf> [November 2016].

Schiarizza, P., Israel, S., Heffernan, S., Boulton, A., Bligh, J., Bell, K., Bayliss, S., Macauley, J., Bluemel, B., Zuber, J., Friedman, R.M., Orchard, M.J. and Poulton, T.P. (2013): Bedrock geology between Thuya and Woodjam creeks, south-central British Columbia, NTS 92P/7, 8, 9, 10, 14, 15, 16; 93A/2, 3, 6; BC Ministry of Energy and Mines, BC Geological Survey, Open File 2013-05, 4 sheets, 1:100 000 scale, <http://www.empr.gov.bc.ca/mining/geoscience/publications catalogue/openfiles/2013/pages/2013-5.aspx> [November 2016].

Shen, P., Hattori, K., Pan, H., Jackson, S. and Seitmuratova, E. (2015): Oxidation condition and metal fertility of granitic magmas: zircon trace-element data from porphyry Cu deposits in the Central Asian orogenic belt; Economic Geology, v. 110, p. 1861–1878.

Sillitoe, R.H. (1973): The tops and bottoms of porphyry copper deposits; Economic Geology, v. 68, p. 799-815.

Sillitoe, R.H. (2010): Porphyry copper systems; Economic Geology, v. 105, p. 3–41.

Streck, M.J. and Dilles, J.H. (1998): Sulfur evolution of oxidized arc magmas as recorded in apatite from a porphyry copper batholith; Geology, v. 26, p. 523–526.